Table 14. *Observed and calculated frequencies of space-group types in the cubic geometric class $m\bar{3}$; the cohort is the geometric class*

Space group No.	Symbol	Arithmetic class	[2]	[m]	Frequency Observed	Calculated
200	$Pm\bar{3}$	62	3	3	0	0
201	$Pn\bar{3}$	62	3	0	0	0
202	$Fm\bar{3}$	63	2	2	1	1
203	$Fd\bar{3}$	63	2	0	0	1
204	$Im\bar{3}$	64	2	2	2	1
205	$Pa\bar{3}$	62	0	0	19	19
206	$Ia\bar{3}$	64	2	0	3	1

Parameter value with program-estimated standard deviation

	Value	E.s.d.	
Coefficient of [2]	−1·82	0·37	
R_2	0·12	—	$R_{rms} = 0·22$
Scaled deviance	2·7	3·2	
Degrees of freedom	5	—	

The coefficients of [m] and of arithmetic class are not significant.

I am indebted to Professor Theo Hahn for help in the understanding of symmetry elements and of their representation in *International Tables for Crystallography*, and to my colleagues at the Cambridge Crystallographic Data Centre, particularly Drs Frank Allen and David Watson, for making available programs and carrying out the searches necessary for this work.

References

ALLEN, F. H., BELLARD, S., BRICE, M. D., CARTWRIGHT, B. A., DOUBLEDAY, A., HIGGS, H., HUMMELINK, T., HUMMELINK-PETERS, B. G., KENNARD, O., MOTHERWELL, W. D. S., RODGERS, J. R. & WATSON, D. G. (1979). *Acta Cryst.* B**35**, 2331-2339.

BAKER, R. J. & NELDER, J. A. (1978). *The GLIM System.* Release 3. Numerical Algorithms Group, Oxford.

DONOHUE, J. (1985). *Acta Cryst.* A**41**, 203-204.

HAHN, TH. (1987). Editor. *International Tables for Crystallography*, Vol. A. *Space-Group Symmetry*, 2nd ed. Dordrecht: Kluwer Academic Publishers. Reprinted with corrections 1989.

KITAIGORODSKY, A. (1945). *J. Phys. USSR*, **9**, 351-352.

KITAIGORODSKY, A. I. (1955). *Organic Crystallochemistry.* Moscow: Izd. Akad. Nauk USSR. (In Russian.)

RAMAKUMAR, S. (1988). National Seminar on Crystallography, Varanasi, India, 15 December 1988.

WILSON, A. J. C. (1976). *Acta Cryst.* A**32**, 994-996.

WILSON, A. J. C. (1980). *Acta Cryst.* A**36**, 937-944.

WILSON, A. J. C. (1987). *Acta Cryst.* A**43**, C289.

WILSON, A. J. C. (1988*a*). *Acta Cryst.* A**44**, 715-724.

WILSON, A. J. C. (1988*b*). National Seminar on Crystallography, Varanasi, India, 15 December 1988.

WONDRATSCHEK, H. (1987). *Introduction to Space-Group Symmetry.* In *International Tables for Crystallography*, Vol. A. *Space-Group Symmetry*, 2nd ed., edited by TH. HAHN, pp. 712-735. Dordrecht: Kluwer Academic Publishers. Reprinted with corrections 1989.

Acta Cryst. (1990). A**46**, 754-763

X-ray Birefringence and Dichroism in Lithium Niobate, $LiNbO_3$

BY A. PETCOV, A. KIRFEL AND K. FISCHER

Universität des Saarlandes, FR Kristallographie, D-6600 Saarbrücken 11, Federal Republic of Germany

(*Received* 6 *March* 1990; *accepted* 18 *April* 1990)

Abstract

Accurate synchrotron-radiation X-ray transmission measurements have been carried out on hexagonal $LiNbO_3$ in the vicinity of the Nb K-absorption edge ($E = 18·986$ keV). The experiments were performed on the two-axis diffractometer at HASYLAB in dedicated mode of DORIS II (3·7 GeV). Single-crystal wafers cut perpendicular to [10.0] were rotated around the monochromatized beam using an experimental set up analogous to the optical polarizing microscope. Both the horizontally and vertically polarized components of the transmitted radiation were recorded at the same time and analysed in terms of a classical optical model derived from the Jones calculus. Fits to the observations yielded agreement indices between 0·013 and 0·052 supporting the applicability of the model to X-ray energies. X-ray

0108-7673/90/090754-10$03.00

dichroism and birefringence are proved to occur at resonance energies, and all findings show the possibility of simultaneous assessment of anisotropies of the real and imaginary parts of the refractive index in a uniaxial crystal. They also indicate that the polarization of the transmitted radiation (of suitable energy) can be varied considerably in dependence of crystal thickness and orientation with respect to the polarization direction of the incident radiation. For special structures like $LiNbO_3$, where the tensorial scattering factor of the edge atom (Nb) is invariant against the symmetry operations of the space group, the method yields also the energy-dependent anisotropy of the anomalous-dispersion corrections, f' and f'', in the same experiment.

Introduction

For X-ray energies the polarizability and the closely related refractive index of a crystal are usually approximated by scalars providing invariance of transmission and scattering against the crystal's orientation with respect to the polarization of the incident radiation. While this approximation is often justified, it may not suffice at frequencies near the absorption edge of a constituent element (hereafter referred to as 'edge atom'). In the early 1960's the polarization dependence of X-ray absorption in crystals was demonstrated by several authors using conventional radiation sources (Alexander, Feller, Fraenkel & Perel, 1965; Brümmer & Dräger, 1966). Such sources were also used in the studies of X-ray polarization phenomena by Hart (1978) and Hart & Rodriguez (1981). The availability of highly polarized synchrotron radiation which can be fine tuned over a wide range of energies has renewed the interest in absorption studies, especially in the XANES and EXAFS regions. Following the observation of anisotropy effects in the white line of Se in layered WSe_2-2H by Heald & Stern (1977), Cox & Beaumont (1980) reported a significant polarization dependence in the X-ray absorption spectrum of rutile-type ZnF_2, from which they concluded that the edge-atom potential is heavily influenced by the local field created by the surrounding F atoms.

Since then, both X-ray transmission through and diffraction of anisotropic materials have been assessed in the vicinities of K- and L-absorption edges in a number of synchrotron experiments. Important work in this field has been carried out by Templeton & Templeton (1980, 1982, 1985*a*, 1988, 1989) who studied X-ray dichroism (and birefringence), and accordingly the anisotropy of anomalous dispersion in X-ray diffraction. From the latter follows, in agreement with the theoretical work by Dmitrienko (1983, 1984), the possibility of the violation of systematic-absence rules due to screw axes and glide planes. This effect was proved experimentally by Templeton & Templeton (1985*b*, 1987), Kirfel, Petcov, Fischer & Eichhorn (1988, 1989), Kirfel & Eichhorn (1989), Kirfel & Petcov (1989) and Kirfel, Petcov, Jauch & Palmer (1989).

The experimental results obtained so far indicate that the polarization phenomena can be related to the chemical bonding of the edge atom in an anisotropic chemical environment. This leads to preferred orientations of unoccupied electronic levels which can manifest themselves in polarization dependence of the real and imaginary parts of the refractive index. In that case the X-ray optical properties are to be described by second-rank tensors within the dipole approximation (Kolpakov, Bushuyev & Kuz'min, 1978)

For ferroelectric lithium niobate, $LiNbO_3$, space group $R3c$, a first investigation of the Nb K-edge anisotropy of the anomalous-dispersion-correction terms, f' and f'', which are directly related to the real and imaginary parts of the refractive index, was undertaken by Bonse & Henning (1986). With the hexagonal c_0 axis perpendicular to the beam, but parallel or normal to the synchrotron plane, they performed absorption and interferometric measurements yielding a significant dependence of the transmission on the crystals orientation.

In the present work we have studied the Nb K-edge absorption of $LiNbO_3$ in more detail aiming to prove simultaneously the occurrence of dichroism and birefringence. Experimental data were collected on the two-axis diffractometer (Bonse & Fischer, 1981), installed at HASYLAB/DESY, for a variety of energies using a sample-rotation technique (χ scan). In order to assess the validity of a classical optical model, the description of the transmission through a plate of a dichroic and birefringent uniaxial crystal was derived from the Jones calculus (Jones, 1941, 1942, 1947, 1948, 1956; Hurwitz & Jones 1941). This calculus provides a very concise method to describe interactions of polarized light with optical components. A recent application to light reflection from minerals is given by Gunter (1989). In the present study, the correlation of the observed and calculated intensities of both the horizontally and vertically polarized components of the transmitted radiation as function of the angle χ (between the c_0 axis and the synchrotron plane) is analysed, and the physical relevance of the derived model parameters is discussed.

The optical model

An electromagnetic plane wave of elliptical polarization propagating parallel to Y in the laboratory system (Fig. 1)

$$D = D_0 \exp\{i[\omega t - (\omega/c)\bar{n}y]\} \qquad (1)$$

can be represented by the column vector of dielectric

displacement

$$|D_0\rangle = \begin{pmatrix} A_{0x} \\ A_{0z} \end{pmatrix}. \tag{2}$$

A_{0x} and A_{0z} are complex numbers, and $\bar{n} = n - i\mu c/2\omega$ is the complex refractive index of the medium. With the formalism introduced by Jones (1941) along with the notation of Blume & Kistner (1968), the global effect of a plane-parallel optical element on $|D_0\rangle$ is described by a 2×2 matrix (with complex elements)

$$\hat{M} = \begin{pmatrix} M_{xx} & M_{xz} \\ M_{zx} & M_{zz} \end{pmatrix}. \tag{3}$$

The transmitted wave is then

$$|D\rangle = \hat{M}|D_0\rangle. \tag{4}$$

In order to specify $\hat{M}$ for a particular optical device, a differential operator

$$\hat{N} = (\mathrm{d}\hat{M}/\mathrm{d}y)\hat{M}^{-1} \tag{5}$$

is formed which models the intensive properties of the medium by a linear combination of up to eight elementary $\hat{\theta}$ matrices (Jones, 1948). The first two matrices introduce changes in the phase and intensity of the beam (corresponding to the action of the mean refractive index and the absorption coefficient, respectively). The remaining six matrices denote changes in its polarization.

For a linear dichroic and linear birefringent crystal only four of these matrices contribute, namely

$$\begin{aligned}
\hat{\Theta}_1 &= -i\frac{\omega}{c}\frac{1}{2}(n_z + n_x)\begin{pmatrix} 1 & 0 \\ 0 & 1 \end{pmatrix}, \\
\hat{\Theta}_2 &= -\frac{1}{4}(\mu_z + \mu_x)\begin{pmatrix} 1 & 0 \\ 0 & 1 \end{pmatrix}, \\
\hat{\Theta}_5 &= -i\frac{\omega}{c}\frac{1}{2}(n_z - n_x)\begin{pmatrix} -1 & 0 \\ 0 & 1 \end{pmatrix}, \\
\hat{\Theta}_6 &= -\frac{1}{4}(\mu_z - \mu_x)\begin{pmatrix} 1 & 0 \\ 0 & -1 \end{pmatrix}.
\end{aligned} \tag{6}$$

n_x, n_z are the real parts of the ordinary and extraordinary refractive index, respectively. The corresponding absorption coefficients are μ_x, μ_z.

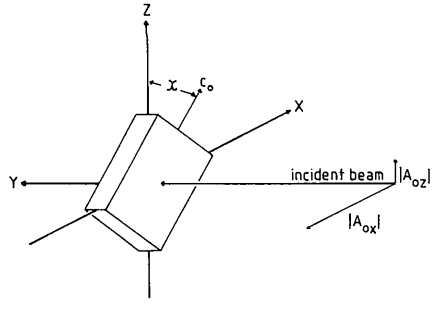

Fig. 1. The crystal plate in the laboratory system. The χ rotation is indicated.

Thus,

$$\hat{N} = \hat{\Theta}_1 + \hat{\Theta}_2 + \hat{\Theta}_5 + \hat{\Theta}_6 \tag{7}$$

and since $\hat{M}$ and $\hat{N}$ are related by

$$\hat{M} = \exp(\hat{N}y) \tag{8}$$

a crystal plate of thickness d is characterized by a Jones matrix

$$\hat{M}_0 = \begin{pmatrix} \exp\left(-i\frac{\omega}{c}n_x d - \frac{1}{2}\mu_x d\right) & 0 \\ 0 & \exp\left(-i\frac{\omega}{c}n_z d - \frac{1}{2}\mu_z d\right) \end{pmatrix}. \tag{9}$$

Rotation of the optical device around the incoming beam by an angle χ transforms the $\hat{M}_0$ matrix into

$$\hat{M}(\chi) = \hat{S}(\chi)\hat{M}_0\hat{S}(-\chi), \tag{10}$$

where $\hat{S}(\chi)$ is the rotation matrix

$$\hat{S}(\chi) = \begin{pmatrix} \cos\chi & -\sin\chi \\ \sin\chi & \cos\chi \end{pmatrix}. \tag{11}$$

Thus, for the transmitted plane wave

$$|D(\chi)\rangle = \hat{M}(\chi)|D_0\rangle, \tag{12}$$

the corresponding total intensity $I_t(\chi)$ is

$$\begin{aligned}
I_t(\chi) &= \langle D^*(\chi)|D(\chi)\rangle = \langle D_0^*|\hat{S}(\chi)\hat{M}_0^\dagger\hat{M}_0\hat{S}(-\chi)|D_0\rangle \\
&= \exp(-\mu_x d)[|A_{0x}|^2 \\
&\quad \times\{\cos^2\chi + \exp[-(\mu_z - \mu_x)d]\sin^2\chi\} \\
&\quad + |A_{0z}|^2\{\sin^2\chi + \exp[-(\mu_z - \mu_x)d]\cos^2\chi\} \\
&\quad + \mathrm{Re}(A_{0x}A_{0z}^*)\{1 - \exp[-(\mu_z - \mu_x)d]\sin 2\chi\}]
\end{aligned} \tag{13}$$

(* and † denote complex and Hermitian conjugates respectively).

$I_t(\chi)$ is periodic in π exhibiting one maximum per period. The modulation of $I_t(\chi)$ depends solely on the anisotropy in μ, *i.e.* the dichroism $\Delta\mu = \mu_z - \mu_x$.

Analysers transmitting waves linearly polarized along X and Z, respectively, are described by the matrices

$$\hat{P}_x = \begin{pmatrix} 1 & 0 \\ 0 & 0 \end{pmatrix} \text{ and } \hat{P}_z = \begin{pmatrix} 0 & 0 \\ 0 & 1 \end{pmatrix}. \tag{14}$$

Then, orthogonally polarized waves transmitted by the combinations of the optical element (*i.e.* the crystal) with each analyser are

$$\begin{aligned}
|D_x(\chi)\rangle &= \hat{P}_x|D(\chi)\rangle = \hat{P}_x\hat{M}(\chi)|D_0\rangle \\
\text{and} \\
|D_z(\chi)\rangle &= \hat{P}_z|D(\chi)\rangle = \hat{P}_z\hat{M}(\chi)|D_0\rangle.
\end{aligned} \tag{15}$$

From $\hat{P}_x^\dagger \hat{P}_x = \hat{P}_x$ and $\hat{P}_z^\dagger \hat{P}_z = \hat{P}_z$, the resulting intensities are given by

$$\begin{aligned} I_x(\chi) &= \langle D_x^*(\chi)|D_x(\chi)\rangle \\ &= \langle D_0^*|\hat{S}(\chi)\hat{M}_0^\dagger \hat{S}(-\chi)\hat{P}_x\hat{S}(\chi)\hat{M}_0\hat{S}(-\chi)|D_0\rangle \\ I_z(\chi) &= \langle D_z^*(\chi)|D_z(\chi)\rangle \\ &= \langle D_0^*|\hat{S}(\chi)\hat{M}_0^\dagger \hat{S}(-\chi)\hat{P}_z\hat{S}(\chi)\hat{M}_0\hat{S}(-\chi)|D_0\rangle, \end{aligned} \tag{16}$$

whose sum equals $I_t(\chi)$ of (13) as can be easily verified. $I_x(\chi)$ and $I_z(\chi)$ are also π-periodic exhibiting, however, in general two maxima of different heights:

$$\begin{aligned} I_x(\chi) &= \exp(-\mu_x d) \\ &\quad \times |A_{0x} - (1-\exp\{-[i(\omega/c)\Delta n - \tfrac{1}{2}\Delta\mu]d\}) \\ &\quad \times (A_{0x}\sin^2\chi - A_{0z}\sin\chi\cos\chi)|^2 \\ I_z(\chi) &= \exp(-\mu_x d) \\ &\quad \times |A_{0z} + (1-\exp\{-[i(\omega/c)\Delta n - \tfrac{1}{2}\Delta\mu]d\}) \\ &\quad \times (A_{0x}\sin\chi\cos\chi - A_{0z}\cos^2\chi)|^2. \end{aligned} \tag{17}$$

Contrary to the total transmitted intensity, which must be invariant against birefringence, the χ patterns of these intensity functions depend explicitly on both the dichroism, $\Delta\mu$, and the anisotropy of the real part of the refractive index, *i.e.* the birefringence $\Delta n = n_z - n_x$.

Thus, observing the transmitted intensities, I_x and I_z, corresponds to studying the crystal plate under the polarizing microscope with parallel and crossed polarizers, respectively.

Equations (17) can be simplified assuming the incident radiation to be linearly polarized in the horizontal plane, *i.e.* $A_{0z} = 0$. Then, one obtains explicitly:

$$\begin{aligned} I_x(\chi) &= \exp(-\mu_x d)|A_{0x}|^2[\cos^2\chi + \exp(-\Delta\mu d)\sin^2\chi \\ &\quad - T\sin^2\chi\cos^2\chi] \\ I_z(\chi) &= \exp(-\mu_x d)|A_{0x}|^2 T\sin^2\chi\cos^2\chi \end{aligned} \tag{18}$$

with $T = 1 - 2\cos[(\omega/c)\Delta n d]\exp(-\frac{1}{2}\Delta\mu d)$. Some more or less trivial consequences of (18) can be derived in agreement with expectations:

(i) $I_x(\chi) = \exp(-\mu d)|A_{0x}|^2$ and $I_z(\chi) = 0$ for $\Delta\mu = \Delta n = 0$;

(ii) $I_z(\chi)$ vanishes for $\chi = 0, \pm\frac{1}{2}\pi, \pi$ and $d = 0$;

(iii) an optical device consisting of two identical crystal plates rotated against each other by 90° is characterized by the Jones matrix

$$\begin{aligned} \hat{M}_{1,2}(\chi) &= \hat{S}(\chi - 90°)\hat{M}_0\hat{S}(-\chi - 90°)\hat{M}_0 \\ &= \exp\left\{-\left[i\frac{\omega}{c}(n_z + n_x) - \frac{1}{2}(\mu_z + \mu_x)\right]d\right\} \\ &\quad \times \begin{pmatrix} 1 & 0 \\ 0 & 1 \end{pmatrix}, \end{aligned} \tag{19}$$

which is χ independent. Thus, no transmission anisotropy can be exhibited by such a combination.

The structure of stoichiometric $LiNbO_3$

Lithium niobate, $LiNbO_3$, is one of the strongest known ferroelectrics and has been the object of numerous experimental studies and applications owing to its outstanding electro-optical properties (Känzig, 1957).

Under normal conditions, $LiNbO_3$ crystallizes in space group $R3c$, with $Z = 6$, Nb and Li in 6(a) (3), and O in 18(b) (1) for the hexagonal setting (a = 5·14739, c = 13·8649 Å). The structure is described in detail by Abrahams & Marsh (1986).

Here it suffices to emphasize the NbO_6 octahedra in which all Nb atoms are displaced along c_0 by 0·27 Å from the centre of gravity of the O atoms. This shift leads to a considerably anisotropic environment for Nb with greatly differing Nb–O distances of 1·8762 (7) and 2·1296 (9) Å. The Li atom is also displaced from the centre of a trigonal oxygen arrangement resulting in an LiO_3 pyramid of 0·45 Å height. Both cation displacements point in the same direction giving rise to permanent 'molecular' electric dipole moments parallel to c_0, and the collective effect of the polar structure accounts for the ferroelectricity.

Similarly, the parallel orientations of all Nb environments favour a macroscopic manifestation of polarization phenomena, since any anisotropy of the Nb potential is multiplied by the number of NbO_6 octahedra in the crystal.

Sample preparation

6×8 mm single-crystal slices of about 500 μm thickness cut perpendicular to [10.0] were provided by the Fraunhofer Institut für Physikalische Messtechnik, Freiburg, Federal Republic of Germany. They were lapped with SiC and polished with Syton down to 55–70 μm. Plane parallelity was checked by micrometer measurements yielding maximum deviations of 3°. In order to ensure mechanical stability and easy manipulation, the wafers were then glued onto 150 μm thick glass plates. A final check of each sample under an optical polarizing microscope gave no evidence of domains, scratches or other macroscopic defects.

Experimental

All experiments were carried out during dedicated beam time (DORIS II operated at 3·7 GeV, critical energy 9 keV) on the two-axis diffractometer installed at beam line G3 in HASYLAB (Bonse & Fischer, 1981).

The radiation was monochromatized by a water-cooled symmetric Ge(511) double-crystal

arrangement with fixed exit. Taking into account both the natural divergence of the synchrotron radiation and the divergence of the electron beam at G3 (Brefeld, 1989), the total divergence of the 19 keV component is about 0·15 mrad, yielding a theoretical resolution of the monochromator of 9 eV. The intensity of higher harmonics was well below the 1% level.

In the four-bunch mode the maximal injected current was close to 100 mA with the frequency of synchrotron flashes 4 MHz.

The experimental set up is shown schematically in Fig. 2. A hollow turntable (χ circle) was mounted on the diffractometer, and the χ axis was aligned to coincide with the direction of the monochromatic X-ray beam. Optimal homogeneity of the primary radiation was achieved by selecting a 2×2 mm cross section from a 10×10 mm beam entering the monochromator.

The samples consisted of one to four wafers which could be mounted on two sample holders allowing for parallel or perpendicular orientations. The optical fine adjustment of the wafers (perpendicular to the χ axis) was performed using a laser beam.

The horizontally and vertically polarized components of the incident radiation were monitored by a polarimeter (Smend, Schaupp, Czerwinski, Millhouse & Schenk-Strauss, 1984) equipped with an Si-powder-coated Kapton foil as scatterer. The same material was used behind the rotating sample for registering the dominant horizontally polarized component of the transmitted radiation, I_x. The much weaker vertically polarized component I_z was observed by measuring, in the horizontal plane, the intensity maximum of a single-crystal Ge(777) Bragg reflection whose 2θ equalled 88·8° for the Nb K edge ($E=18{\cdot}986$ keV).

Owing to this fortuitous circumstance, I_z^t could be investigated almost independently of I_x^t and with a calculated energy resolution of 2·9 eV ($\Delta E/E=1{\cdot}5\times10^{-4}$). Provided Bragg reflection in the crystal can be excluded or assumed negligible, the experiment is an analogue to the optical polarizing microscope. The χ rotation around the beam corresponds to a rotation of the microscope's turntable, and with the synchrotron acting as polarizer and the Ge crystal as analyser, the observation of I_z^t is equivalent to light-transmission studies under crossed polarizers.

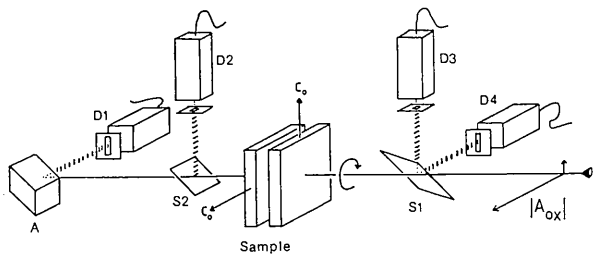

Fig. 2. Experimental set up. $D1,\ldots,D4$: NaI detectors ($D1$ registering count rates $C1$ and $C5$); $S1, S2$: scattering foils; A: Ge(777) analyser.

χ scans

The measuring system, based on the CAMAC-bus, was controlled by a PDP 11/73 and included on-line normalization and graphical representation of the χ-scan results. Thus, a valuable check of the intensity curve and of the stability of the experimental conditions was provided.

The most interesting energy range for the investigation of polarization phenomena in $LiNbO_3$ is in the near-edge region encompassing the Nb absorption pre-peak (Fig. 3). At this energy a salient transition between orthogonal resonances had been observed in previous measurements (Petcov, Kirfel & Fischer, 1988). On the energy scale chosen in Fig. 3, the absorption pre-peak corresponds to the Nb K-edge energy (18·986 keV).

The experimental procedure at a given energy consisted of:

(i) optimization of primary-beam intensity by tilting the second monochromator crystal using a piezoelectric drive;

(ii) fine adjustment of the Ge(777) reflection by means of a high-resolution rotation stage (Bonse & Teworte, 1982) carrying the analyser crystal;

(iii) the χ scan: full rotation of the sample around the beam with angular increments $\Delta\chi=5$ or 10°, respectively. At each χ position:

5 to 15 s determination of the count rates of the horizontally and vertically polarized photons before $[C_3(\chi), C_4(\chi)]$ and after the sample $[C_1(\chi), C_2(\chi)$, see Fig. 2], as well as of the higher harmonic contributions, $C_5(\chi)$;

on-line calculation and display of the normalized transmitted intensities

$$I_x^{obs}(\chi)=C_2(\chi)/C_3(\chi)$$
$$I_z^{obs}(\chi)=C_1(\chi)/C_3(\chi) \qquad (20)$$

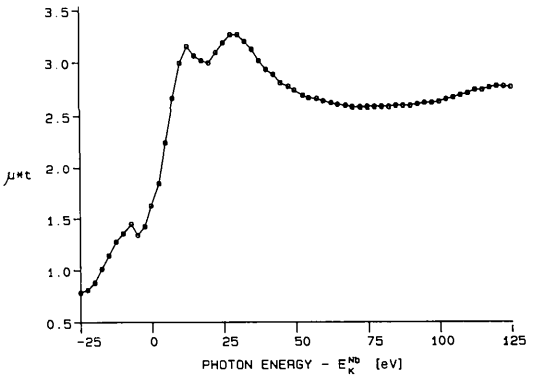

Fig. 3. Near-edge absorption spectrum of $LiNbO_3$ wafer with c_0 in the horizontal plane.

which are thus corrected for the temporal decrease and instabilities of the primary-beam intensity;

(iv) repetition of (iii) if counting statistics were unsatisfactory.

The experiments comprised:

(1) 33 χ scans of equidistantly distributed energies between 18·971 and 19·005 keV using a sample of three wafers with parallel c_0 axes (data sets: IH1–IH33 and IV1–IV33).

(2) At the energy of maximum anisotropy effects ($E = 18{\cdot}992$ keV) χ scans using samples with varying numbers and relative orientations of wafers in order to elucidate the origin of the χ-dependent transmission effects.

(3) χ scans at different heights of the two-axis diffractometer relative to the electron orbit, *i.e.* with assumedly different elliptical polarization of the incident radiation.

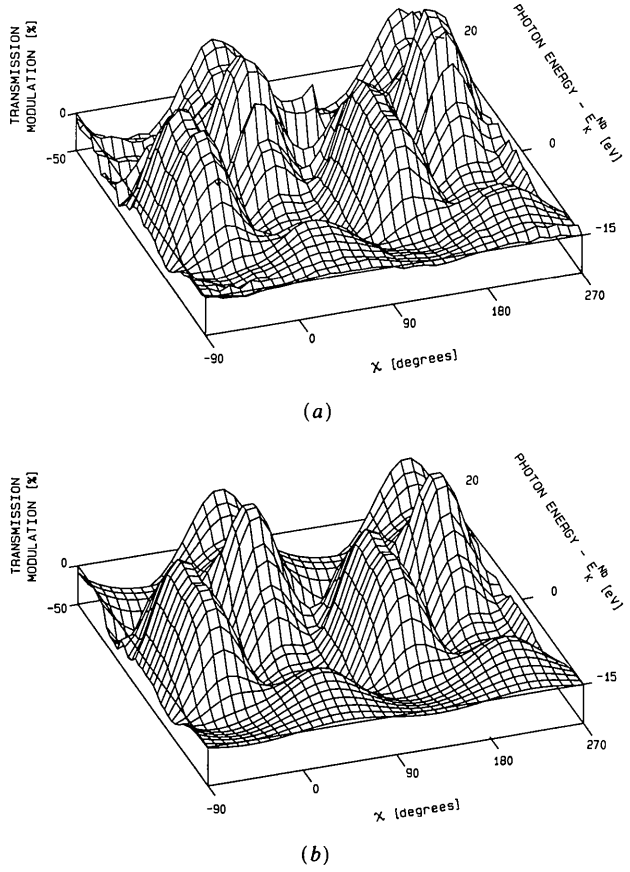

Fig. 4. Modulation of the vertically polarized transmitted radiation, $\Delta I_z(\chi, E)/\langle I_z(E)\rangle$: (*a*) observed, (*b*) calculated.

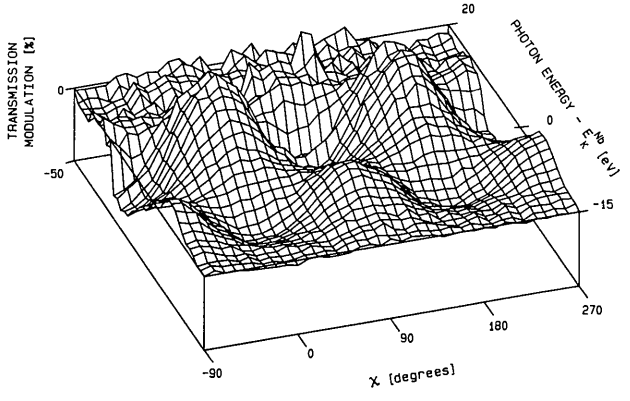

Fig. 5. Observed modulation of the horizontally polarized transmitted radiation, $\Delta I_x(\chi, E)/\langle I_x(E)\rangle$.

Qualitative results

The 33 observed transmission patterns, $I_z^{obs}(\chi)$, are summarized in Fig. 4(*a*) in the form of $\Delta I_z/\langle I_z\rangle$, where $\langle I_z\rangle$ is the mean value and $\Delta I_z = I_z - \langle I_z\rangle$ the variation of the intensity of the vertically polarized component. Fig. 4(*a*) gives further evidence of X-ray optical polarization phenomena in the vicinity of an absorption edge. In the 3D representation of $I_z^{obs}(\chi)$, a smooth transition between orthogonal resonances, each associated with a pair of maxima, can be recognized around E_K^{Nb}. Evidence of birefringence is given in the patterns exhibiting four maxima.

Though present, these are unobservable in the corresponding plot of $I_x^{obs}(\chi)$ (Fig. 5), which is dominated by the energy-dependent anisotropy of absorption in agreement with the earlier observed transmission patterns (Petcov, Kirfel & Fischer, 1988). For $E = 18{\cdot}992$ keV and a sample consisting of two wafers of about equal thickness and orthogonal c_0 orientation, the $I_z^{obs}(\chi)$ and $I_x^{obs}(\chi)$ modulations turned out to be insignificant [in agreement with (19)], but were essentially reproduced upon changing the mutual orientation of the wafers to anti-parallel. Increasing the sample thickness by combining up to four parallel oriented wafers resulted in increasing modulations of $I_z^{obs}(\chi)$ from 40 to 90%, accompanied by the unavoidable severe decrease of the mean transmission. Since any manipulation of the sample required closing and reopening the beam shutter (thus switching the heat load on the monochromator on and off), minor changes of the radiation energy could not be excluded so that more detailed quantitative results of the thickness effect cannot be given. Nevertheless, all findings indicated the presence of a true polarization effect varying with sample orientation and/or thickness. Finally, significant changes of the $I_z^{obs}(\chi)$ pattern upon varying the instrument height within a few mm were not detected.

Data analysis

The observed $I_z^{obs}(\chi)$ and $I_x^{obs}(\chi)$ of the data sets IV and IH were analysed according to the optical model outlined above.

The $\hat{M}(\chi)$ matrix was parametrized as

$$\hat{M}(\chi) = c\begin{pmatrix} \cos^2\chi + \exp(-a-ib)\sin^2\chi & [1-\exp(-a-ib)]\sin\chi\cos\chi \\ [1-\exp(-a-ib)]\sin\chi\cos\chi & \sin^2\chi + \exp(-a-ib)\cos^2\chi \end{pmatrix}, \quad (21)$$

$a = \frac{1}{2}\Delta\mu d$, $b = (\omega/c)\Delta n d$ and $c = \exp(-\frac{1}{2}\mu_x d)$ are adjustable constants for fixed energy.

The elliptically polarized synchrotron beam has a sectional pattern with horizontal major axis (Shurcliff, 1966) and is described by the column vector

$$|D_0\rangle = A_0\begin{pmatrix} 1 \\ ip \end{pmatrix}, \quad (22)$$

where $|p| \leq 1$ is related to the degree of the linear horizontal polarization L_x,

$$L_x = (I_x - I_z)/(I_x + I_z) = (1-p^2)/(1+p^2). \quad (23)$$

The calculated components of the transmitted wave [see (17)] are

$$\begin{aligned} I_x^{\text{cal}}(\chi) &= c^2|[1-\exp(-a-ib)] \\ &\quad \times (ip\sin\chi\cos\chi - \sin^2\chi) + 1|^2 \\ I_z^{\text{cal}}(\chi) &= c^2|[1-\exp(-a-ib)] \\ &\quad \times (\sin\chi\cos\chi - ip\cos^2\chi) + ip|^2. \end{aligned} \quad (24)$$

For each of the 33 investigated energies these two model intensity functions were adjusted simultaneously to the normalized observed transmission data $I_x^{\text{obs}}(\chi)$ and $I_z^{\text{obs}}(\chi)$ (20). The non-linear optimization procedure of Davidon, Fletcher & Powell (James & Roos, 1987) was applied to the χ^2 function:

$$S = \sum \frac{|I_x^{\text{obs}}(\chi) - I_x^{\text{cal}}(\chi)|^2}{I_x^{\text{cal}}(\chi)} + \sum \frac{|rI_z^{\text{obs}}(\chi) - I_z^{\text{cal}}(\chi)|^2}{I_z^{\text{cal}}(\chi)}, \quad (25)$$

where r is an adjustable scaling factor taking into account the different efficiencies of the two detection systems.

Convergence was rapid and all elements of the correlation matrix were typically below 0·4. Since p enters (24) as p^2, a certain ambiguity exists with respect to its sign which defines the handedness of the synchrotron radiation. This difficulty was overcome by choosing that sign which complies with smooth variations of the other parameters as functions of the photon energy.

As examples for the obtained fit results, Fig. 6 depicts experimental points together with the corresponding model curves at four different energies.

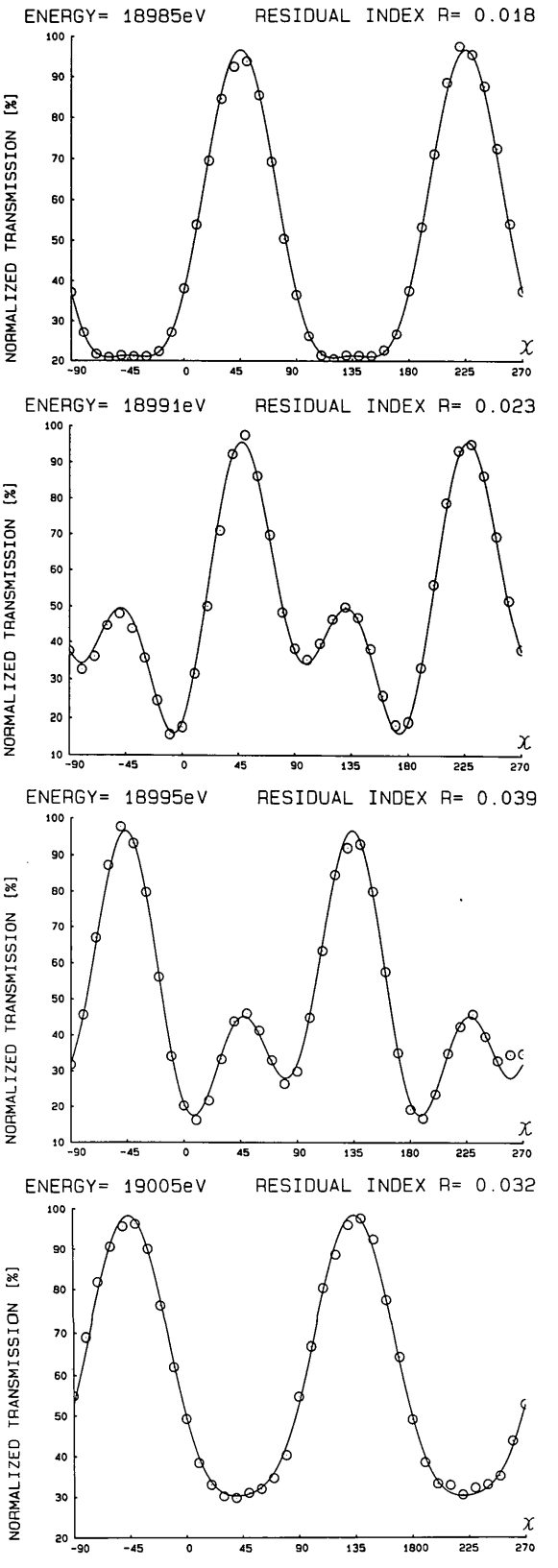

Fig. 6. Intensity of the vertically polarized transmitted radiation, $I_z(\chi)$. Experimental points and model curves at: (*a*) 18·990, (*b*) 18·992, (*c*) 18·994 and (*d*) 18·997 keV.

The agreement between the observations and the model is expressed by the index

$$R=\frac{\sum|I_x^{obs}(\chi)-I_x^{cal}(\chi)|^2}{\sum[I_x^{cal}(\chi)]^2}+\frac{\sum|rI_z^{obs}(\chi)-I_z^{cal}(\chi)|^2}{\sum[I_z^{cal}(\chi)]^2}, \quad (26)$$

which varied between 0·013 and 0·052. The overall agreement can also be judged by comparing the transmission surfaces of the observations (Fig. 4*a*) and of the adjusted model (Fig. 4*b*). Discrepancies between model and observations are most probably due to instabilities of the beam, *i.e.* small energy variations occurring mainly at the end of a synchrotron-radiation run.

The energy-dependent birefringence, Δn, and dichroism, $\Delta\mu$, calculated from the refined parameters $a(E)$ and $b(E)$ are shown in Figs. 7(*a*), (*b*). According to Fig. 7, maximum values of $\Delta n=-0{\cdot}11\times10^{-7}$ and $\Delta\mu=53{\cdot}6\ cm^{-1}$ were calculated. The Δn value corresponds (mod 2π) to a phase lag of about $60°\ mm^{-1}$ between the components of the transmitted radiation.

For $LiNbO_3$ ($Z=6$), a and b are related to the real and imaginary parts of the complex scattering factors for $|D_x\rangle$ and $|D_z\rangle$ by

$$a=6\lambda r_0(d/V)\ \mathrm{Im}\,(f_z^{Nb}-f_x^{Nb})$$
$$b=6\lambda r_0(d/V)\ \mathrm{Re}\,(f_z^{Nb}-f_x^{Nb}) \quad (27)$$

(V = unit-cell volume, r_0 = classical electron radius). Thus, a and b describe also the anisotropy of the anomalous-dispersion corrections, f' and f'', and from (27) result the maximum observed values $\Delta f'=\mathrm{Re}\,(f_z^{Nb}-f_x^{Nb})=-0{\cdot}30(8)$ and $\Delta f''=\mathrm{Im}\,(f_z^{Nb}-f_x^{Nb})=0{\cdot}70(1)$. These figures may be compared with $f'=-6{\cdot}1$ e and $f''=1{\cdot}6$ e of metallic niobium taken from the interferometric measurements of Hart & Siddons (1981).

The χ-dependent degree of horizontal linear polarization of the transmitted radiation, $L_x(\chi)$, (23), can be calculated either from the experimental data or from the refined parameters. Examples are given in Fig. 8, where $L_x(\chi)$ is depicted for two samples investigated at the same energy. These curves show that - without substantial loss of transmitted intensity

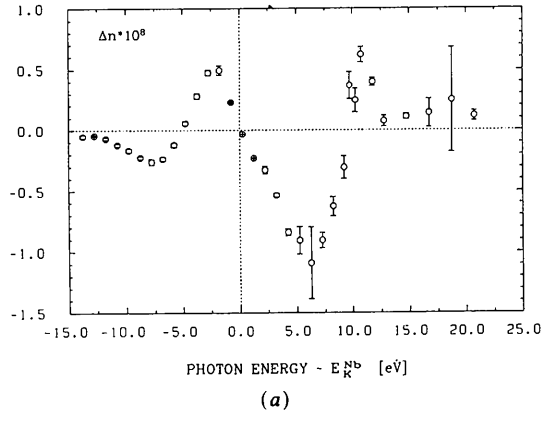

(*a*)

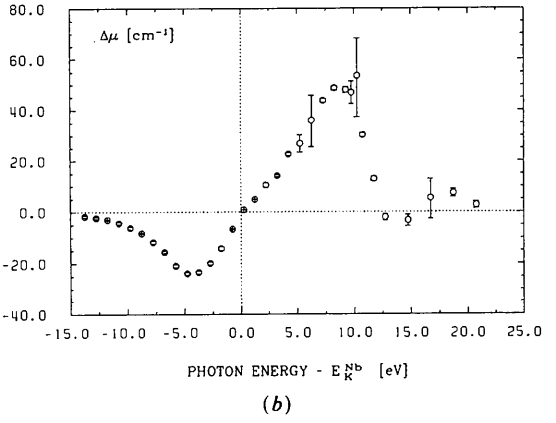

(*b*)

Fig. 7. Energy dependence of dichroism, $\Delta\mu$, and birefringence, Δn, in the vicinity of the Nb K-absorption edge ($E=18{\cdot}986$ keV).

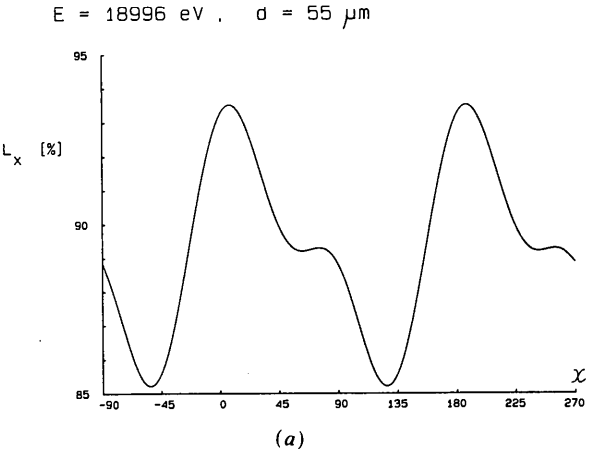

(*a*)

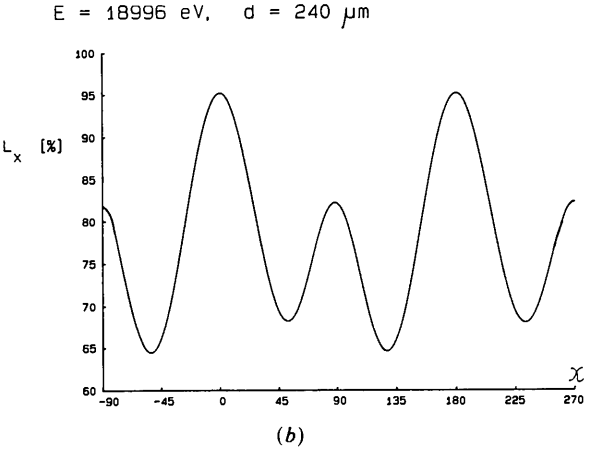

(*b*)

Fig. 8. Degree of linear polarization, $L_x(\chi)$, of the radiation transmitted through samples of: (*a*) 55 and (*b*) 240 μm thickness.

$-L_x$ can be varied over a wide range by an appropriate choice of crystal orientation and thickness.

Discussion

The observed dependence of the transmitted intensities, $I_x^t(\chi)$ and $I_z^t(\chi)$, on both radiation energy and crystal orientation is a direct proof of the occurrence of X-ray dichroism and birefringence in a uniaxial crystal. Both effects arise in the XANES region, when the energy of the incident radiation matches the resonance energy required for the excitement of a 'core' electron into an unoccupied (but allowed) state of preferred orientation. Thus, we discuss resonance phenomena which are to be distinguished from (energy-independent) diffraction-induced dichroism and birefringence in perfect crystals [being observable even for cubic symmetry - Belyakov & Dmitrienko (1989)]. Studying resonance-induced polarized absorption spectra and birefringence under proper experimental conditions, one can elucidate the symmetry and orientation of above-Fermi-edge levels and contribute to investigations on the electronic structures in a crystal.

In the case of $LiNbO_3$, two such states of apparently orthogonal orientations were resolved. Their excitements provide X-ray optical uniaxiality in each case, but change the crystal from being optically positive to negative within a few electronvolts. This finding is of interest in terms of comparison with electronic-band-structure calculations. In the present context, however, emphasis was put on the analytical description of the effects on the basis of a classical optical model. The model is formulated in concise form by application of the Jones calculus. Given the anisotropic complex refractive index along with the polarization of the radiation, the model predicts both intensity and polarization of the transmitted radiation as a function of thickness and orientation of the crystal plate. This approach is justified by the agreement between the experimental results and the calculations giving credit to the applicability of the optical model to X-ray energies. It appears therefore feasible to handle the transmission of polarized X-rays through an X-ray optically anisotropic medium by a concise matrix algorithm. Such an algorithm should be useful, for example, in calculations of intensities of space-group extinct ('forbidden') Bragg reflections caused by polarization-dependent resonance scattering (anisotropic anomalous dispersion) which are simultaneously affected by anisotropy of absorption.

Another consequence of the results involves the interpretation of polarized absorption spectra obtained from a single crystal with orientation χ. It is obvious that in the case of elliptically polarized radiation the total transmitted intensity, $I_t(\chi)$, recorded by an ionization chamber or by direct-beam measurement with a detector, can differ from the intensity component of the, say, horizontally polarized radiation, $I_x(\chi)$. This intensity should be measured in front and after the sample for the correct determination of the corresponding absorption coefficient μ_x (Petcov, Kirfel & Fischer, 1988). Employing $I_t(\chi)$ instead of $I_x(\chi)$ in the calculation of μ_x introduces an error $\Delta\mu_x = I_z(\chi)/[dI_x(\chi)]$ that cannot be generally neglected (d = sample thickness). The relative error

$$\Delta\mu_x(\chi)/\mu_x(\chi) = I_z(\chi)/[I_x(\chi)d\mu_x(\chi)] \quad (28)$$

can amount to a few percent, as estimated for $LiNbO_3$ with, for example, $I_z/I_x = 0{\cdot}2$, $\mu_x d = 3$.

Such errors are less important in a XANES study of the projected density of states which is approximately proportional to $\mu_x(E)$. In an EXAFS study, however, which is based on the relative change of $\mu_x(E)$ with respect to the unperturbed absorption by the edge atoms, $\mu_0(E)$, the amplitude of the EXAFS oscillation is typically smaller than 0·1. Since the absolute error introduced into the function is $\Delta\mu_x(E)/\mu_x(E)$, it should be noted that polarization-dependent EXAFS results may be significantly biased by neglect of the proper experimental conditions.

The observed X-ray dichroism and birefringence result from a projection of the atomic scattering factors (or X-ray susceptibilities) along the propagation direction of the radiation. They reflect averages over all atoms in the unit cell so that detailed information about the individual atom is generally lost. In cubic crystals, for example, the symmetry precludes anisotropy of absorption. In uniaxial crystals of special structures, however, where a scattering-factor tensor of the edge atom is invariant against the symmetry operations of the space group, the anisotropy of the macroscopic refractive index is proportional to the anisotropy of the edge atom's anomalous dispersion. This applies to $LiNbO_3$ in which all Nb atoms are located on threefold axes parallel to c_0. For such a structure it is possible to assess not only $f''(E)$ and $\Delta f''(E)$, but also $\Delta f'(E)$ directly and simultaneously in the same experiment *via* the observation of dichroism and birefringence.

As to the relation between the derived $\Delta f'(E)$ and $\Delta f''(E)$, they can be expected to obey the Kramers–Kronig dispersion relation. Under the limiting condition that $\Delta f''$ vanishes outside the investigated energy range, the real part calculated by the Kramers–Kronig transformation disagreed with the observed $\Delta f'(E)$. The latter as well as $\Delta f''(E)$ are, however, in qualitative agreement with the interferometer and transmission results of Bonse & Henning (1986). We assume therefore that the data included in the Kramers–Kronig integration were insufficient.

Finally, we wish to emphasize the dependence of the data quality on stable radiation properties. Similar measurements carried out during high-energy operation of Doris II (5·3 GeV, no beam stabilization)

yielded unsatisfactory results owing to considerable beam instabilities. Hence, the present work profited from a period of excellent ring operation with stable beam and electron current life times of up to 4h.

Applications of the method to other non-cubic structures with comparable properties are most likely to corroborate the optical model, and further experiments with new substances are planned.

Financial support, granted by the Bundesminister für Forschung und Technologie, is gratefully acknowledged.

References

ABRAHAMS, S. C. & MARSH, P. (1986). *Acta Cryst.* B**42**, 61-68.

ALEXANDER, E., FELLER, S., FRAENKEL, B. S. & PEREL, J. (1965). *Nuovo Cimento*, **35**, 311-312.

BELYAKOV, V. A. & DMITRIENKO, V. E. (1989). *Nucl. Instrum. Methods*, **282**, 526-528.

BLUME, M. & KISTNER, O. C. (1968). *Phys. Rev.* **171**, 417-425.

BONSE, U. & FISCHER, K. (1981). *Nucl. Instrum. Methods*, **190**, 593-603.

BONSE, U. & HENNING, A. (1986). *Nucl. Instrum. Methods*, A**246**, 814-816.

BONSE, U. & TEWORTE, R. (1982). *J. Phys. E*, **15**, 187-190.

BREFELD, W. (1989). Private communication.

BRÜMMER, O. & DRÄGER, G. (1966). *Phys. Status Solidi*, **14**, K175-K179.

COX, A. D. & BEAUMONT, J. H. (1980). *Philos. Mag.* B**42**, 115-126.

DMITRIENKO, V. E. (1983). *Acta Cryst.* A**39**, 29-35.

DMITRIENKO, V. E. (1984). *Acta Cryst.* A**40**, 89-95.

GUNTER, M. E. (1989). *Eur. J. Mineral.* **1**, 801-814.

HART, M. (1978). *Philos. Mag.* B**38**, 41-56.

HART, M. & RODRIGUEZ, R. D. (1981). *Philos. Mag.* B**43**, 321-332.

HART, M. & SIDDONS, D. P. (1981). *Proc. R. Soc. London Ser. A*, **376**, 465-482.

HEALD, S. M. & STERN, E. A. (1977). *Phys. Rev. B*, **16**, 5549-5559.

HURWITZ, H. & JONES, R. C. (1941). *J. Opt. Soc. Am.* **31**, 493-499.

JAMES, F. & ROOS, M. (1987). *MINUIT* Program. CERN Computer Centre, Program Library No. D506. CERN, Geneva, Switzerland.

JONES, R. C. (1941). *J. Opt. Soc. Am.* **31**, 488-493, 500-503.

JONES, R. C. (1942). *J. Opt. Soc. Am.* **32**, 486-493.

JONES, R. C. (1947). *J. Opt. Soc. Am.* **37**, 107-110, 110-112.

JONES, R. C. (1948). *J. Opt. Soc. Am.* **38**, 671-685.

JONES, R. C. (1956). *J. Opt. Soc. Am.* **46**, 126-131.

KÄNZIG, W. (1957). *Ferroelectrics and Antiferroelectrics.* London: Academic Press.

KIRFEL, A. & EICHHORN, K. (1989). HASYLAB/DESY Jahresbericht, pp. 383-384. HASYLAB, Hamburg, Federal Republic of Germany.

KIRFEL, A. & PETCOV, A. (1989). HASYLAB/DESY Jahresbericht, pp. 385-386. HASYLAB, Hamburg, Federal Republic of Germany.

KIRFEL, A., PETCOV, A., FISCHER, K. & EICHHORN, K. (1988). *Z. Kristallogr.* **185**, 160-161.

KIRFEL, A., PETCOV, A., FISCHER, K. & EICHHORN, K. (1989). *Z. Kristallogr.* **186**, 158-161.

KIRFEL, A., PETCOV, A., JAUCH, W. & PALMER, A. (1989). HASYLAB/DESY Jahresbericht, pp. 387-388. HASYLAB, Hamburg, Federal Republic of Germany.

KOLPAKOV, A. V., BUSHUYEV, V. A. & KUZ'MIN, R. N. (1978). *Sov. Phys. Usp.* **21** (11), 959-977.

PETCOV, A., KIRFEL, A. & FISCHER, K. (1988). *Z. Naturforsch. Teil A*, **43**, 388-390.

SHURCLIFF, W. A. (1966). *Polarized Light.* Harvard Univ. Press.

SMEND, F., SCHAUPP, D., CZERWINSKI, H., MILLHOUSE, A. H. & SCHENK-STRAUSS, H. (1984). DESY Internal Report SR-84-003. DESY/HASYLAB, Hamburg, Federal Republic of Germany.

TEMPLETON, D. H. & TEMPLETON, L. K. (1980). *Acta Cryst.* A**36**, 436-442.

TEMPLETON, D. H. & TEMPLETON, L. K. (1982). *Acta Cryst.* A**38**, 62-67.

TEMPLETON, D. H. & TEMPLETON, L. K. (1985*a*). *Acta Cryst.* A**41**, 133-142.

TEMPLETON, D. H. & TEMPLETON, L. K. (1985*b*). *Acta Cryst.* A**41**, 365-371.

TEMPLETON, D. H. & TEMPLETON, L. K. (1987). *Acta Cryst.* A**43**, 573-574.

TEMPLETON, D. H. & TEMPLETON, L. K. (1988). *Acta Cryst.* A**44**, 1045-1051.

TEMPLETON, D. H. & TEMPLETON, L. K. (1989). *Acta Cryst.* A**45**, 39-42.

Acta Cryst. (1990). A**46**, 763-772

On Differentiation of the Scattering Matrix in Dynamical Transmission Electron Diffraction

BY S. SPEER AND J. C. H. SPENCE

Department of Physics, Arizona State University, Tempe, AZ 85287, *USA*

AND E. IHRIG

Department of Mathematics, Arizona State University, Tempe, AZ 85287, *USA*

(*Received* 3 *January* 1990; *accepted* 9 *May* 1990)

Abstract

High-energy transmission electron diffraction from thin crystals under conditions of multiple scattering is considered. An expression is derived for the Jacobian of the scattering-matrix mapping, containing all partial derivatives of the scattering-matrix elements with respect to structure-matrix elements. (This structure matrix describes the scattering crystal and incident-beam direction). These results may be used

0108-7673/90/090763-10$03.00